A&A 366, 771–787 (2001)
DOI: 10.1051/0004-6361:20000333

Astronomy & Astrophysics

The Hamburg/SAO survey for emission–line galaxies

IV. The fourth list of 119 galaxies

A. Y. Kniazev[1,8], D. Engels[2], S. A. Pustilnik[1,8], A. V. Ugryumov[1,8], T. F. Kniazeva[1], A. G. Pramsky[1], N. Brosch[3], H.-J. Hagen[2], U. Hopp[4], Y. I. Izotov[5], V. A. Lipovetsky[1,⋆], J. Masegosa[6], I. Márquez[6], and J.-M. Martin[7]

[1] Special Astrophysical Observatory, Nizhnij Arkhyz, Karachai-Circessia 369167, Russia
[2] Hamburger Sternwarte, Gojenbergsweg 112, 21029 Hamburg, Germany
[3] Wise Observatory, Tel-Aviv University, Tel-Aviv 69978, Israel
[4] Universitätssternwarte München, Scheiner Str. 1, 81679 München, Germany
[5] Main Astronomical Observatory, Goloseevo, Kiev-127 03680, Ukraine
[6] Instituto de Astrofisica de Andalucia, CSIC, Aptdo. 3004, 18080 Granada, Spain
[7] Département de Radioastronomie ARPEGES, Observatoire de Paris, 92195 Meudon Cedex, France
[8] Isaac Newton Institute of Chile, SAO Branch

Received 17 August 2000 / Accepted 23 November 2000

Abstract. We present the fourth list with results** of the Hamburg/SAO Survey for Emission-Line Galaxies (HSS hereafter, SAO – Special Astrophysical Observatory, Russia). The list is a result of the follow-up spectroscopy conducted with the 6 m SAO RAS telescope in 1998, 1999 and 2000. The data of this snap-shot spectroscopy survey confirmed 127 emission-line objects out of 176 observed candidates and allowed their quantitative spectral classification. We could classify 76 emission-line objects as BCG/HII galaxies or probable BCGs, 8 – as QSOs, 2 – as Seyfert galaxies, 2 – as super-associations in a subluminous spiral and an irregular galaxy, and 37 as low-excitation objects – either starburst nuclei (SBN), or dwarf amorphous nuclei starburst galaxies (DANS). We could not classify 2 ELGs. Furthermore, for 5 galaxies we did not detect any significant emission lines. For 91 emission-line galaxies, the redshifts and/or line intensities are determined for the first time. Of the remaining 28 previously known ELGs we give either improved data on the line intensities or some independent measurements. The candidates were taken from three different samples selected by different criteria. Among our first priority candidates we achieved a detection rate of emission-line objects (ELGs + QSOs) of 68%, among which 51% are BCGs. Observations of a random selected sample among our second priority candidates showed that only ≈10% are BCGs. We found that the confirmed BCGs have usually a blue colour ($(B-R) < 1\overset{\mathrm{m}}{.}0$) and a non-stellar appearance in the APM database. Our third sample is comprised of second priority candidates fulfilling these criteria derived from the APM. Follow-up spectroscopy of a small subsample indicates that the expected detection rate for BCGs is ≈40%.

Key words. surveys – galaxies: fundamental parameters – galaxies: distances and redshifts – galaxies: starburst – galaxies: compact – quasars: redshifts

1. Introduction

The main goal of the Hamburg/SAO Survey for Emission-Line Galaxies (HSS) is the search for emission-line galaxies (ELG) in order to create a new deep sample of blue compact/HII galaxies (BCG) in a large area of the sky with a size of the order 1700 square degrees. Another important goal of this work is to search for new extremely low-metallicity galaxies. The search is carried out on the objective prism plates of the Hamburg Quasar Survey (Hagen et al. 1995). The boundaries of our survey are $7^{\mathrm{h}}20^{\mathrm{m}}$ to $17^{\mathrm{h}}40^{\mathrm{m}}$ in right ascension and +35° to +50° in declination, which bridges the gap between the zones of the Second Byurakan Survey (SBS; Markarian et al. 1983; Stepanian 1994) and the region covered by the Case (Pesch et al. 1995) survey. The SBS is situated at

Send offprint requests to: A. Y. Kniazev, e-mail: akn@sao.ru
⋆ Deceased 22 September 1996.
** Tables 3 to 8 are only available in electronic form at the CDS via anonymous ftp to cdsarc.u-strasbg.fr (130.79.128.5) or via
http://cdsweb.u-strasbg.fr/cgi-bin/qcat?J/A+A/366/771
Figures A1 and A12 are only available in electronic form at http://www.edpsciences.org

Table 1. Summary of the samples observed and breakdown of the classifications after follow-up spectroscopy

Candidate Classification	Sample	N	BCGs	Other ELGs	QSO	Galaxies without ELs	Stars	Not Classified
First priority	new	113	47	24	7	3	7	25
	already known	26	19	7	–	–	–	–
	Total	139	66	31	7	3	7	25
Second priority	6 m observations	26	1	10	1	1	9	4
	2.2 m observations	17	3	2	–	1	3	8
	Random (total)	43	4	12	1	2	12	12
	APM selected (total)	11	7	4	–	–	–	–
Objects presented in this paper		176	74	45	8	4	16	29

$\alpha = 7^{\rm h}40^{\rm m} \div 17^{\rm h}20^{\rm m}$, $\delta = +49^\circ \div +61^\circ$, while the Case zone corresponds to the region with $\alpha = 8^{\rm h}00^{\rm m} \div 16^{\rm h}20^{\rm m}$, $\delta = +29^\circ \div +38^\circ$. After combination of the four BCG samples coming from the SBS (Izotov et al. 1993a, 1993b; Thuan et al. 1994; Pustilnik et al. 1995), from the Case survey (Salzer et al. 1995; Ugryumov 1997; Ugryumov et al. 1998), from the HSS, and from part of the Heidelberg Void survey sample (Popescu et al. 1996), a large Northern BCG Sample covering about 1 steradian will be available.

In the Papers I and II (Ugryumov et al. 1999; Pustilnik et al. 1999) we presented results of our survey in the region between $\delta = 40{-}50^\circ$, while in Paper III (Hopp et al. 2000) and the present paper results from the strip $\delta = 35{-}40^\circ$ are given. Forthcoming papers will complete the follow-up spectroscopy in these two regions.

The article is organized as follows. In Sect. 2 we will review our selection method and present the samples discussed here. In Sect. 3 we describe the spectroscopic observations and the data reduction. In Sect. 4 the results of the observations are presented in several tables. In Sect. 5 we briefly discuss the new data and summarize the current state of the Hamburg/SAO survey. Throughout this paper a Hubble constant $H_0 = 75$ km s^{-1} Mpc^{-1} is used.

2. Selection method

The basic ideas of the HSS and its selection methods of ELG candidates are described in Paper I. The final selection was slightly modified to improve significantly the detection rate of ELGs in the follow-up spectroscopy as described in Paper II. As it was outlined in Paper I, the selection procedure provided us finally with two candidate lists (first and second priorities): 1st – objects showing a clear density peak near λ5000 Å and blue continuum in the Hamburg Quasar Survey objective-prism spectra scanned with high resolution; 2nd – candidates with a blue continuum but without prominent emission features or candidates with indications of emission peaks but with an unusual continuum shape. In short, the ELG candidate selection criteria applied are a blue or flat continuum (near λ4000 Å) and the presence of strong or moderate [OIII] $\lambda\lambda$ 4959, 5007 Å emission lines recognized on digitized prism spectra. Candidates accepted had B-magnitudes in the range $16^{\rm m}{-}19\overset{\rm m}{.}5$.

Based on the experience with a training sample of BCGs drawn from the Second Byurakan Survey (see Paper I for details) the first priority candidates were considered as highly probable HII/BCG type emission galaxies. The follow-up snap-shot spectroscopy confirmed that among all detected ELGs this type of galaxies constitutes up to 70–80%. Thus, our main goal to create a large new sample of BCG/HII-galaxies in the HSS region is achieved by follow-up spectroscopy of the full sample of first priority candidates.

In this paper we will present the results for follow-up spectroscopy of three samples listed in Table 1. The first sample is made up by 139 first priority candidates in the strip $\delta = 35{-}40^\circ$ of which 26 are known ELGs. For the latter galaxies additional spectra were required to improve their classification.

The other two samples were drawn from the second priority candidates of the same strip. We found in Paper I that the detection efficiency of HII/BCG galaxies is rather low among them, prohibiting follow-up spectroscopy of all second priority candidates. Moreover, the second priority objects are about twice as numerous than the first priority ones. At the faint end, this sample is also dominated by candidates selected because of noise peaks in their objective prism spectra. We created therefore a random selected sample of 43 second priority objects from this strip matching in its magnitude distribution the sample of first priority candidates. These objects make up 10% of the second priority sample in the magnitude range of the first priority candidates. We obtained follow-up spectroscopy of all objects to study the general content and to determine the fraction of BCGs in this sample.

The third sample (referred to as *APM Selected* in Table 1) was created by applying additional selection criteria to the second priority candidates to increase the detection efficiency for BCG/HII-galaxies among them. These criteria and the results of follow-up spectroscopy are described in Sect. 4.2.2.

Table 2. Log of observations at the SAO 6 m telescope

Run No (1)	Date (2)			Instrument (3)	Grating [grooves/mm] (4)	Wavelength Range [Å] (5)	Dispersion [Å/pixel] (6)
1	17–19	Dec.	1998	CCD, SP–124	300	3600–7800	4.6
2	08–13	Feb.	1999	CCD, LSS	325	3600–7800	4.6
3	02	Sep.	1999	CCD, LSS	650	3700–6100	2.4
	04	Sep.	1999	CCD, LSS	325	3600–7800	4.6
4	02	Feb.	2000	CCD, LSS	650	3700–6100	2.4

3. Spectral observations and data reduction

3.1. Observations

All results presented below have been obtained by observations with the Russian 6 m telescope, mainly in the snap-shot mode during 4 runs between December 1998 and February 2000. The spectrograph SP-124 attached to the Nasmyth-1 focus of the telescope was used during the first run. We used a grating with 300 grooves/mm (see log of observations in Table 2) and a long slit of $2'' \times 40''$. The scale along the slit was $0.4''$/pixel.

The Long-Slit Spectrograph (LSS in Table 2) (Afanasiev et al. 1995) attached to the telescope prime focus was used during the remaining 3 runs. Most of the long-slit spectra ($1\farcs2$–$2\farcs0 \times 180''$) were obtained with a grating of 325 grooves/mm, giving a dispersion of 4.6 Å/pixel. Additional data were obtained with a grating of 650 grooves/mm giving a dispersion of 2.4 Å/pixel. The scale along the slit was $0.39''$/pixel. For all observations we used the Photometrics CCD-detector PM1024 with 24×24 μm pixel size.

Normally, short exposures were used (2−5 min) in order to detect strong emission lines, to measure redshifts and make a first classification. Reference spectra of an Ar–Ne–He lamp were recorded before or after each observation to provide a wavelength calibration. Spectrophotometric standard stars from Oke (1990) and Bohlin (1996) were observed for flux calibration at least twice a night. All observations and data acquisition have been conducted under the `NICE` software package by Kniazev & Shergin (1995) in the MIDAS[1] environment.

Part of the second priority candidates was observed with the 2.2 m telescope on Calar Alto in June 1999. These observations will be presented in a forthcoming paper, although we will make use of the results in our analysis below.

3.2. Data reduction

The data reduction was done at SAO with the IRAF[2] and the MIDAS software packages. In all details of the reduction process and the measuring of line parameters we followed the procedures described in Paper III. Since we present a substantial number of objects with redshifts known from earlier publications, we could independently test the quality of our wavelength calibration. The results of these tests indicate that our internal errors σ_V shown in Table 3 are close to the external errors and do not change from run to run.

[1] MIDAS is an acronym for the European Southern Observatory package — Munich Image Data Analysis System.

[2] IRAF is distributed by National Optical Astronomical Observatories, which is operated by the Association of Universities for Research in Astronomy, Inc., under cooperative agreement with the National Science Foundation.

4. Results of follow–up spectroscopy

4.1. First priority candidates

In total 139 first priority candidates have been observed (Table 1). Of them 26 objects were known as ELG before. In particular, seven of them are from our Paper III, for which the classification was either unknown or uncertain. Of these 139 objects 97 (75%) are new or confirmed emission-line galaxies.

4.1.1. Emission-line galaxies

The emission line galaxies observed are listed in Table 3 containing the following information:
Column 1: The object's IAU-type name with the prefix HS.
Column 2: Right ascension for equinox B1950.
Column 3: Declination for equinox B1950. The coordinates were measured on direct plates of the HQS and are accurate to $\sim 2''$ (Hagen et al. 1995).
Column 4: Heliocentric velocity and its rms uncertainty in km s^{-1}.
Column 5: Apparent B-magnitude obtained by calibration of the digitized photoplates with photometric standard stars (Engels et al. 1994), having an rms accuracy of $\sim 0\fm5$ for objects fainter than $m_B = 16\fm0$ (Popescu et al. 1996). Since the algorithm to calibrate the objective prism spectra is optimized for point sources the brightnesses of extended galaxies are underestimated. The resulting systematic uncertainties are expected to be as large as 2 mag (Popescu et al. 1996). For about 1/3 of our objects, B-magnitudes are unavailable at the moment. We present for them blue magnitudes obtained from the APM database. They are marked by a "plus" before the value in the corresponding column. According to our estimate they are systematically brighter by $0\fm92$ than

the B-magnitudes obtained by calibration of the digitized photoplates (rms $1\overset{m}{.}02$). For all objects marked as from Popescu et al. (2000) one may find improved B-magnitudes in Vennik et al. (2000) which we do not list here for the sake of homogeneity.
Column 6: Absolute B-magnitude, calculated from the apparent B-magnitude and the heliocentric velocity. No correction for galactic extinction is made as all objects are located at high galactic latitudes and because the corrections are significantly smaller than the uncertainties of the magnitudes.
Column 7: Preliminary spectral classification type according to the spectral data presented in this article. BCG means that the galaxy possesses a characteristic HII-region spectrum and that the luminosity is low enough. SBN and DANS are galaxies of lower excitation with a corresponding position in line ratio diagrams, as discussed in Paper I. SBN are the brighter fraction of this type. We here follow the notation of Salzer et al. (1989). Seyfert galaxies are separated mainly on diagnostic diagrams as AGN. The criterion of broad lines was also used for the Sy classification. With SA two probable super-association in a spiral and an irregular galaxy are denoted. Two ELGs are difficult to classify. They are coded as NON.
Column 8: One or more alternative names, according to the information from NED[3]. References to other sources of spectral information indicating that a galaxy is an ELG are given in bold face.

The spectra of all emission-line galaxies are shown in Appendix A, which is available only in the electronic version of the journal.

The results of line flux measurements are given in Table 4. It contains the following information:
Column 1: The object's IAU-type name with the prefix HS. By asterisk we note the objects observed during non-photometric conditions.
Column 2: Observed flux (in 10^{-16} erg s^{-1} cm^{-2}) of the Hβ line. For few objects without Hβ emission line the fluxes are given for Hα and marked by a "plus". For several objects observed during non-photometric conditions this parameter is unreliable and marked by (:).
Columns 3–5: The observed flux ratios [OII]/Hβ, [OIII]/Hβ and Hα/Hβ. For few objects without Hβ flux ratios are given for Hα and marked by a "plus".
Columns 6, 7: The observed flux ratios [NII] λ6583 Å/Hα, and ([SII] λ6716 Å + λ6731 Å)/Hα.
Columns 8–10: Equivalent widths of the lines [OII] λ3727 Å, Hβ and [OIII] λ5007 Å. For few objects without detected Hβ emission line the equivalent widths are given for Hα and marked by a "plus".

Among the 97 ELGs observed as first-priority candidates, 66 are classified as BCGs or probable BCGs. Two very faint objects (HS 1134+3640 and HS 1308+3845) are probably super-associations in the dwarf spiral NGC 3755 and in the Im galaxy UGC 8261. Two ELGs are probable LINERs. One candidate is difficult to classify. The remaining 26 ELGs are objects of lower excitation: either starburst nuclei galaxies (SBN and probable SBN) or their lower mass analogs dwarf amorphous nuclear starburst galaxies (DANS or probable DANS).

Below we give notes on several individual objects:

HS 0847+3639: The HS magnitude for this galaxy seems to be too faint. The KUG magnitude (Takase & Miyauchi-Isobe 1993) $B = 15\overset{m}{.}4$ corresponds to $M_B = -19\overset{m}{.}6$ and an SBN classification as given in Table 3.

HS 0934+3629: The $FWHM$s, corrected for instrumental resolution, for Hα and Hβ are ≈1800 km s^{-1} and ≈1400 km s^{-1}, respectively.

HS 1047+3714: Very strong NII line λ6583 Å, Hβ is only seen in absorption.

HS 1116+3951: Uncertain Hα/Hβ ratio because of a cosmic hit on Hα.

HS 1134+3639: Probable low-mass companion of the galaxy NGC 3755 (the distance is ≈230″ or ∼25 kpc).

HS 1134+3640: Possible giant HII-region at the very edge of the SAB(rs)c pec galaxy NGC 3755 with $V_{\rm hel}$ = 1570 km s^{-1}, seen at an inclination angle of ≈60°. The HI-line width at the level of 0.2 of the peak flux value $W_{0.2}$ = 290 km s^{-1} (Huchtmeier & Richter 1989) corresponds to a maximum $V_{\rm rot}$ of ≈150 km s^{-1}. In accordance with the difference in radial velocities (–108 km s^{-1}) of HS 1134+3640 and the dynamical center of NGC 3755, HS 1134+3640 is either an HII-region in NGC 3755, or a companion like HS 1134+3639. The real situation can be checked only if it is determined whether this edge of NGC 3755, corresponds to the receding or approaching spiral arm.

HS 1308+3545: Giant HII-region at the edge of the $B = 16\overset{m}{.}0$ Im galaxy UGC 8261 with $V_{\rm hel}$ = 852 km s^{-1}. Its HI-line width $W_{0.2}$ = 127 km s^{-1} corresponds to a maximum $V_{\rm rot}$ of ≈65 km s^{-1}. This is consistent with the measured difference in the radial velocities of HS 1308+3545 and the dynamical center of the Im galaxy.

HS 1620+4003: The profiles of the OIII-lines λ4959, 5007 Å have a composite structure with a narrow ($FWHM_{5007} = FWHM_{\rm H\beta}$) and broad ($FWHM \approx$ 1800 km s^{-1}) component. The broad to narrow component flux ratio is 1.44.

4.1.2. Quasars

In the course of our follow-up spectroscopy, seven QSOs were discovered with a strong emission line in the wavelength region between 5000 Å and the sensitivity break of the Kodak IIIa-J photoemulsion near 5400 Å. In all of them, we identified Lyα λ1216 redshifted to $z \sim 3$ as the responsible line. These mostly faint quasars are not found by the HQS itself, which focuses on objects with brightnesses $B \leq 17\overset{m}{.}5$ (Hagen et al. 1999). The data for these 7 new high-redshift quasars (and one from the second priority candidates) are presented in Table 5. Finding charts and plots of their spectra can be found on www-site of the Hamburg Quasar Survey (`http://www.hs.uni-hamburg.de/hqs.html`).

[3] `http://nedwww.ipac.caltech.edu/`

4.1.3. Absorption-line galaxies

For three bright non-ELG galaxies (and one from the second priority candidates) the signal-to-noise ratio of our spectra was sufficient to detect absorption lines, allowing the determination of redshifts. The data are presented in Table 6.

4.1.4. Stellar objects

To separate the stars among the objects missing detectable emission lines we cross-correlated a list of the most common stellar features with the observed spectra. In total, 7 objects with definite stellar spectra and redshifts close to zero were identified (and 9 from the second priority candidates). They were classified roughly in categories from definite A-stars to G-stars, with most of them intermediate between A and F. The data for these stars are presented in Table 7.

4.1.5. Not-classified objects

Twenty five non emission-line objects are hard to classify at all. Their continua have too low signal-to-noise ratio to detect trustworthy absorption features, or the EWs of the emission lines are too small.

4.2. Second priority candidates

4.2.1. The random selected sample

From the random selected subsample of second priority candidates we observed twenty six objects during the 6-m telescope runs (mainly those with RA $< 11^{\rm h}$) along with the observations of first priority targets. Altogether we found 12 emission-line objects: one appeared to be a QSO with $z = 3.15$, and the rest are various types of ELGs. They are shown in Tables 3 and 4, respectively, and are marked by †. Nine objects are stars of spectral classes from A to G, with one M-star. One object is an absorption-line galaxy. The remaining four second priority candidates have no (trustworthy) emission lines, and are probably either absorption line galaxies, or various types of stars. They are considered as "not classified" in Table 1. Among the 11 ELGs only one has a spectrum and an absolute magnitude indicative of a BCG/HII-galaxy. The others are either low excitation ELGs like SBN and DANS, or AGN like LINERs or Sy galaxies.

The remaining 17 candidates were observed with the 2.2 m telescope and three probable BCGs were found among them. Preliminary spectral classification type for these objects are shown in the last column of Table 8. Classification of ELGs follows that described for Table 3. "Star" is star-like object with absorptions at zero redshift. "ABS" is a galaxy with detected and identified absorption lines. "NOEM" is an object with no (trustworthy) emission lines detected.

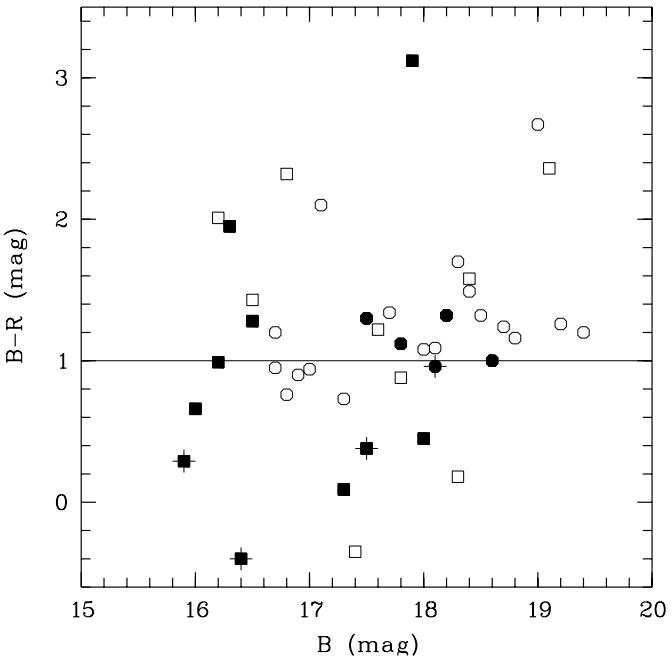

Fig. 1. Colour distribution for the random sample of 42 s priority candidates in the strip $\delta = 35{-}40^{\circ}$ (HS 1423+3945 is not included because its APM-colour is not available). The APM classification is shown by circles for stellar and squares for non-stellar images. The filled symbols show the emission-line objects identified by follow-up spectroscopy. BCG/HII-galaxies are marked by an additional cross. 4 of 5 APM stellar-type emission-line objects are either QSOs or distant luminous galaxies. The horizontal line at $(B-R) = 1\overset{\rm m}{.}0$ shows the colour limit for the selection of BCG candidates among the second priority objects classified as non-stellar in the APM

In total, we found 4 (probable) BCG/HII-galaxies in the random selected sample making up a fraction of ≈10%.

4.2.2. The APM selected sample

To improve the efficiency for the selection of BCGs among the second priority candidates we introduced additional selection criteria using the APM (Irwin 1998) database. An analysis of the spectroscopic classifications of all objects from the random subsample resulted in the following conclusions:

- The second priority candidates classified as BCG/HII based on their slit spectra all have rather blue colours according to the APM database (APM $(B-R) \leq 1\overset{\rm m}{.}0$). In this colour range BCGs constitute about 33% of all second priority objects classified by APM as galaxies (Fig. 1);
- Most of the ELGs of other types are redder than BCGs;
- One BCG of the four newly found is classified in the APM as stellar. Possibly at faint magnitudes some fraction of very compact BCGs are not distinguished by the APM from blue stars. Therefore also the APM information is of no help to discriminate the very compact faint BCGs from blue stars at the faint end of the second priority candidates.

Therefore, having in mind to develop a strategy to pick up as many as possible low-mass BCG/HII-galaxies in the HSS region, but accounting as well for a high enough detection rate, we created a subsample of second priority BCG candidates, which fulfill the following additional criteria:

- APM non-stellar classification, and
- a blue colour ($(B-R) < 1\overset{\mathrm{m}}{.}0$) on the APM.

Of 633 objects from the second priority list in the strip $\delta = 35{-}40^\circ$ 80 candidates were selected by these criteria. Eleven candidates from this additional list were observed by snap-shot spectroscopy. All of them have turned out to be ELGs of various types. 3 of them are certain BCGs, and 4 more are probable BCG/HII-galaxies. They are listed in Table 3 and are marked with ‡.

5. Discussion

5.1. The fourth list

As shown in Table 1, among 104 observed emission-line objects 66 (63%) were classified based on the character of their spectra and their absolute magnitudes as HII/BCGs or probable BCGs. Since the main goal of the HSS is an efficient search for new BCGs, the fraction of this type among all confirmed ELGs of the first priority list (∼68%, or 63% among all emission-line objects) is encouraging.

The distribution of new HSS ELGs in the line-ratio diagrams [OIII] λ 5007/Hβ versus [NII] λ 6583/Hα and [OIII] λ 5007/Hβ versus [OII] λ 3727/[OIII] λ 5007 (see Baldwin et al. 1981; Veilleux & Osterbrock 1987 for details) in general is similar to that shown in Paper I as may be expected since the selection criteria are identical. Several new BCGs with very strong emission lines located in the metal-poor regions of these diagrams were reobserved later with higher signal-to-noise ratio, and four of them (0951+3841, 1028+3843, 1124+3635 and 1309+3806) are found to have $\mathrm{O/H} < 1/10\ (\mathrm{O/H})_\odot$. A full description of the selection procedure for low-metallicity candidates based on snap-shot spectra is given in Kniazev et al. (2000).

The snap-shot spectroscopy of the random selected sample of second priority candidates detected only 4 additional BCG/HII galaxies (≈10%, cf. Table 1). We expect therefore, not much more than ≈60 BCGs among the 633 second priority candidates of the $\delta = 35{-}40^\circ$ strip.

To find these BCGs efficiently we used additional selection criteria based on the APM, which are fulfilled also by most of the BCGs from the first priority list. For this subsample of 80 candidates spectroscopic information is available for 24 objects: 11 were observed by us due to this selection, 10 were already observed as part of the random sample, and for 3 the information was taken from the literature. Altogether 10 BCGs or probable BCGs were found among them. The current estimate of detection rate for BCGs in the APM selected sample is therefore ≈40%.

5.2. Summary of the present status of the survey

Altogether among the objects of first priority in Papers I through IV, we discovered 321 new emission-line objects (20 of them QSOs), and for 55 known ELGs we got quantitative data for their emission lines. Preliminary classification of the 356 ELGs yields 275 (∼77%) confident or probable blue compact/low-mass HII-galaxies. This large fraction demonstrates the high efficiency of this survey to find low-mass galaxies with HII-type spectra on the Hamburg Quasar Survey photoplates. A statistical analysis of this BCG sample, supplemented with galaxies from the SBS, the Case, and the Heidelberg Void samples, is underway. Fourteen more BCGs were found among the second priority candidates.

6. Conclusions

We conducted follow-up spectroscopy of candidates from the Hamburg/SAO Survey for ELGs. Summarizing the results presented, the analysis of the content of various types of objects, and the discussion above, we draw the following conclusions:

- The applied methods to detect ELG candidates on the plates of the Hamburg Quasar Survey give a reasonably high detection rate of emission-line objects: ∼77% in the average, among the first priority candidates as defined in Papers I to IV;
- The high fraction of BCG/HII galaxies among all newly discovered ELGs (about 68% in this paper) is in line with our main goal — to pick up efficiently a deep BCG sample in the sky region under analysis;
- Besides of ELGs we found also 8 new quasars, all with Lyα in the wavelength region 4950−5100 Å (i.e. with $3.15 < z < 3.30$) near the red boundary of the IIIa-J objective prism photoplates. These objects are a byproduct of the survey, as their Lyα line is mistaken for the [OIII] λ 5007 Å line;
- The snap-shot spectroscopy of the random selected sample of second priority candidates shows that BCG/HII-galaxies represent only a small part of the second priority sample (≈10%). Applying additional selection criteria based on APM classification and $(B-R)$ colour allows to extract more reliably these BCGs, except for very compact ones.

Acknowledgements. This work was supported by the grant of the Deutsche Forschungsgemeinschaft No. 436 RUS 17/77/94. U.A.V. is very grateful to the staff of the Hamburg Observatory for their hospitality and kind assistance. Support by the INTAS grant No. 96-0500 was crucial to proceed with the Hamburg/SAO survey declination band centered on +37.5°. We notice that the use of APM facility was extremely valuable for selection methodics of additional candidates to BCGs from the 2nd priority list. The authors are grateful to the referee G. Comte for his useful advises, allowing them to improve the presentation of results. This research has made use of the NASA/IPAC Extragalactic Database (NED) which is operated by the Jet Propulsion Laboratory, California Institute of Technology, under contract with the National Aeronautics and Space Administration.

References

Afanasiev, V. L., Burenkov, A. N., Vlasyuk, V. V., & Drabek, S. V. 1995, SAO RAS internal report No. 247

Augarde, R., Chalabaev, A., Comte, G., Hunth, D., & Maehara, H. 1994, A&AS, 104, 259

Baldwin, J. A., Phillips, M. M., & Terlevich, R. 1981, PASP, 93, 5

Bohlin, R. C. 1996, AJ, 111, 1743

Engels, D., Cordis, L., & Köhler, T. 1994, Proc. IAU Symp. 161, ed. H. T. MacGillivray (Kluwer: Dordrecht), 317

de Grijp, M. H. K., Keel, W. C., Miley, G. K., Goudfrooij, P., & Lub, J. 1992, A&AS, 96, 389

Hagen, H.-J., Groote, D., Engels, D., & Reimers, D. 1995, A&AS, 111, 195

Hagen, H.-J, Engels, D., & Reimers, D. 1999, A&AS, 134, 483

Hopp, U., Engels, D., Green, R., et al. 2000, A&AS, 142, 417, Paper III

Huchra, J. P., Geller, M. J., & Corwin, H. G. Jr. 1995, ApJS, 99, 391

Huchtmeier, W., & Richter, O. 1989, A General Catalog of HI Observations of Galaxies (New York, Springer-Verlag)

Irwin, M. 1998, `http://www.ast.cam.ac.uk/~apmcat/`

Izotov, Yu. I., Guseva, N. G., Lipovetsky, V. A., et al. 1993a, Astron. & Astrophys. Trans., 3, 179

Izotov, Yu. I., Lipovetsky, V. A., & Guseva, N. G. 1993b, in The Feedback of Chemical Evolution on the Stellar Content of Galaxies, ed. D. Alloin, & G. Stasinska, 127

Kniazev, A. Y., Pustilnik, S. A., Ugryumov, A. V., & Kniazeva, T. F. 2000, Astron. Lett., 26, issue 2, 129

Markarian, B. E., Lipovetsky, V. A., & Stepanian, J. A. 1983, Afz, 19, 29

Oke, J. B. 1990, AJ, 99, 1621

Pesch, P., Stephenson, C. B., & MacConnell, D. J. 1995, ApJS, 98, 41

Popescu, C. C., Hopp, U., Hagen, H.-J., & Elsässer, H. 1996, A&AS, 116, 43

Popescu, C. C., & Hopp, U. 2000, A&AS, 142, 247

Pustilnik, S. A., Ugryumov, A. V., Lipovetsky, V. A., Thuan, T. X., & Guseva, N. G. 1995, ApJ, 443, 499

Pustilnik, S. A., Engels, D., Ugryumov, A. V., et al. 1999, A&AS, 135, 299 (Paper II)

Ramella, M., Geller, M. J., Huchra, J. P., & Thorstensen, J. R. 1995, AJ, 109, 1458

Salzer, J. J., MacAlpine, G. M., & Boroson, T. A. 1989, ApJS, 70, 479

Salzer, J. J., Moody, J. W., Rosenberg, J. L., Gregory, S. A., & Newberry, M. V. 1995, AJ, 109, 2376

Schneider, D. P., Schmidt, M., & Gunn, J. E. 1994, AJ, 107, 1245

Stepanian, J. A. 1994, Proc. IAU Symp. 161, ed. H. T. MacGillivray (Kluwer: Dordrecht), 731

Takase, B., & Miyauchi-Isobe, N. 1993, PNAOJ, 3, 169

Thuan, T. X., Izotov, Yu. I., Lipovetsky, V. A., & Pustilnik, S. A. 1994, Proc. ESO/OHP Workshop Dwarf Galaxies, ed. Meylan & Prugniel, 421

Tift, W. C., Kirshner, R. P., Gregory, S. A., & Moody, J. W. 1986, ApJ, 310, 75

Ugryumov, A. V. 1997, Ph.D. Thesis, SAO RAS

Ugryumov, A. V., Pustilnik, S. A., Lipovetsky, V. A., Izotov, Yu. I., & Richter, G. M. 1998, A&AS, 131, 295

Ugryumov, A. V., Engels, D., Lipovetsky, V. A., et al. 1999, A&AS, 135, 511 (Paper I)

Veilleux, S., & Osterbrock, D. E. 1987, ApJS, 63, 295

Vennik, J., Hopp, U., & Popescu, C. C. 2000, A&AS, 142, 399

Weistrop, D., & Downes, R. A. 1991, AJ, 102, 1680

Appendix A: Spectra of emission-line galaxies from the HSS

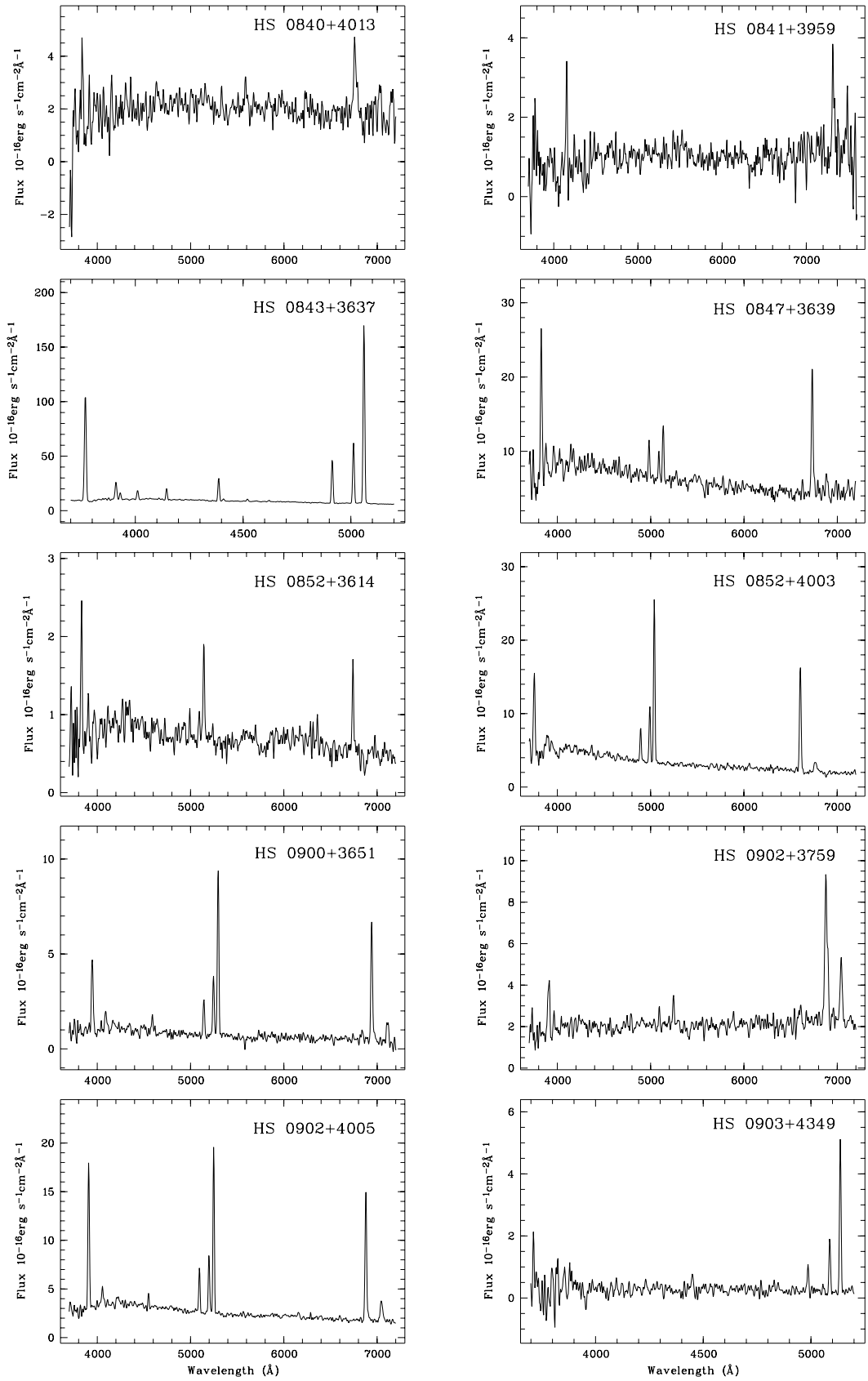

Fig. A2.

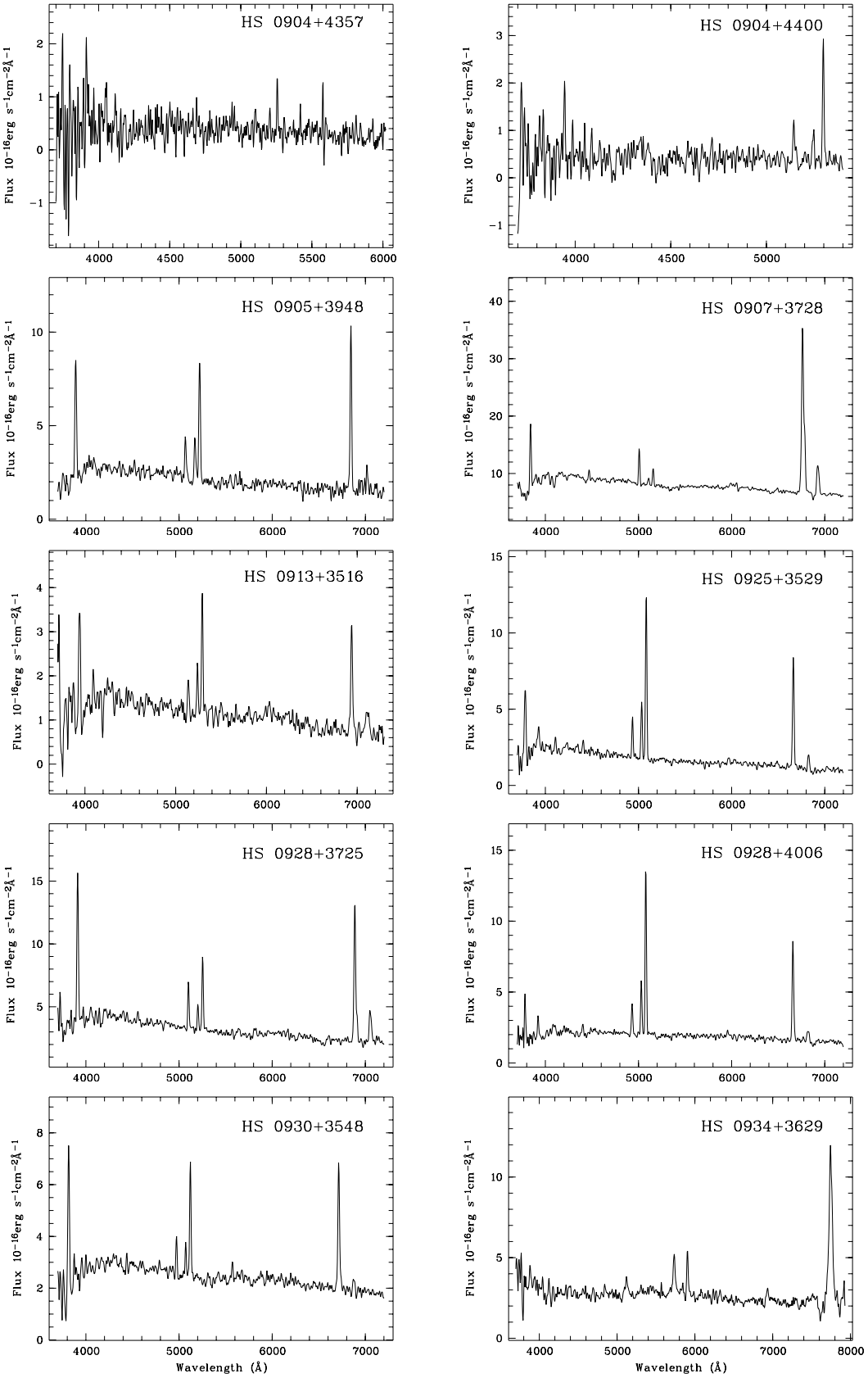
HS 0904+4357
HS 0904+4400
HS 0905+3948
HS 0907+3728
HS 0913+3516
HS 0925+3529
HS 0928+3725
HS 0928+4006
HS 0930+3548
HS 0934+3629
Flux 10⁻¹⁶erg s⁻¹cm⁻²Å⁻¹
Wavelength (Å)

Fig. A3.

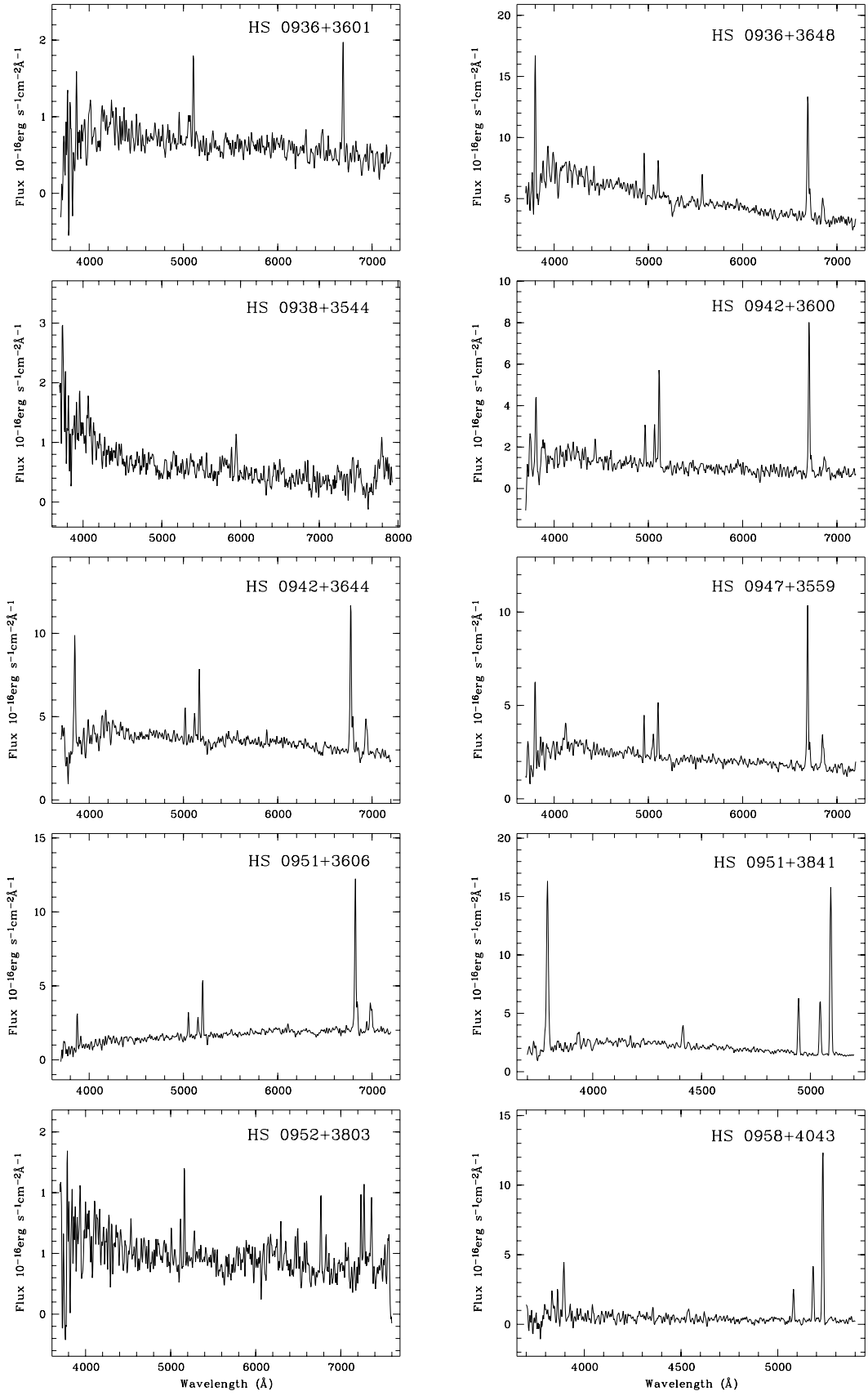
HS 0936+3601
HS 0936+3648
HS 0938+3544
HS 0942+3600
HS 0942+3644
HS 0947+3559
HS 0951+3606
HS 0951+3841
HS 0952+3803
HS 0958+4043
Flux 10⁻¹⁶erg s⁻¹cm⁻²Å⁻¹
Wavelength (Å)

Fig. A4.

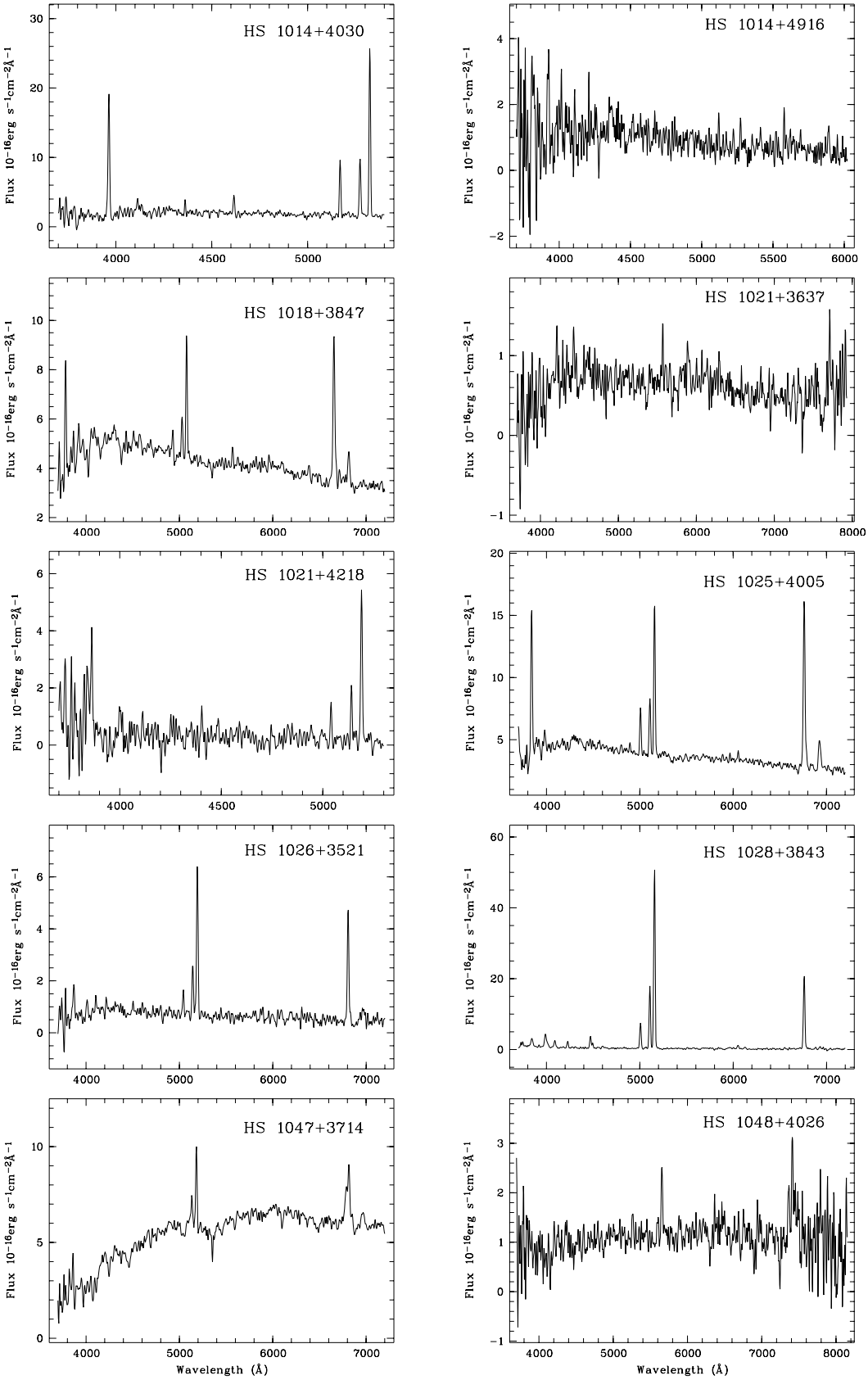
HS 1014+4030
HS 1014+4916
HS 1018+3847
HS 1021+3637
HS 1021+4218
HS 1025+4005
HS 1026+3521
HS 1028+3843
HS 1047+3714
HS 1048+4026
Flux 10⁻¹⁶erg s⁻¹cm⁻²Å⁻¹
Wavelength (Å)

Fig. A5.

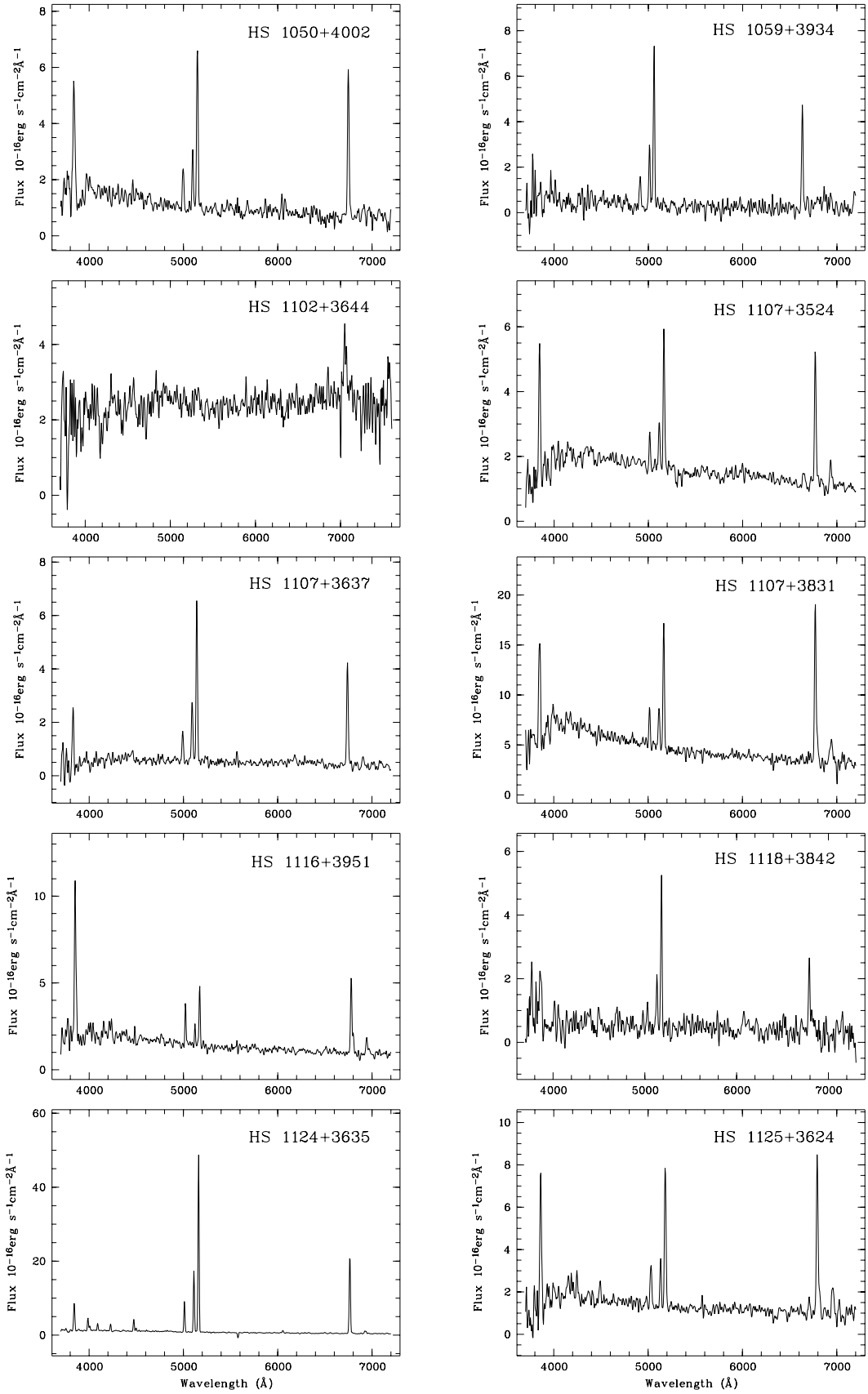
HS 1050+4002
HS 1059+3934
HS 1102+3644
HS 1107+3524
HS 1107+3637
HS 1107+3831
HS 1116+3951
HS 1118+3842
HS 1124+3635
HS 1125+3624
Flux 10⁻¹⁶erg s⁻¹cm⁻²Å⁻¹
Wavelength (Å)

Fig. A6.

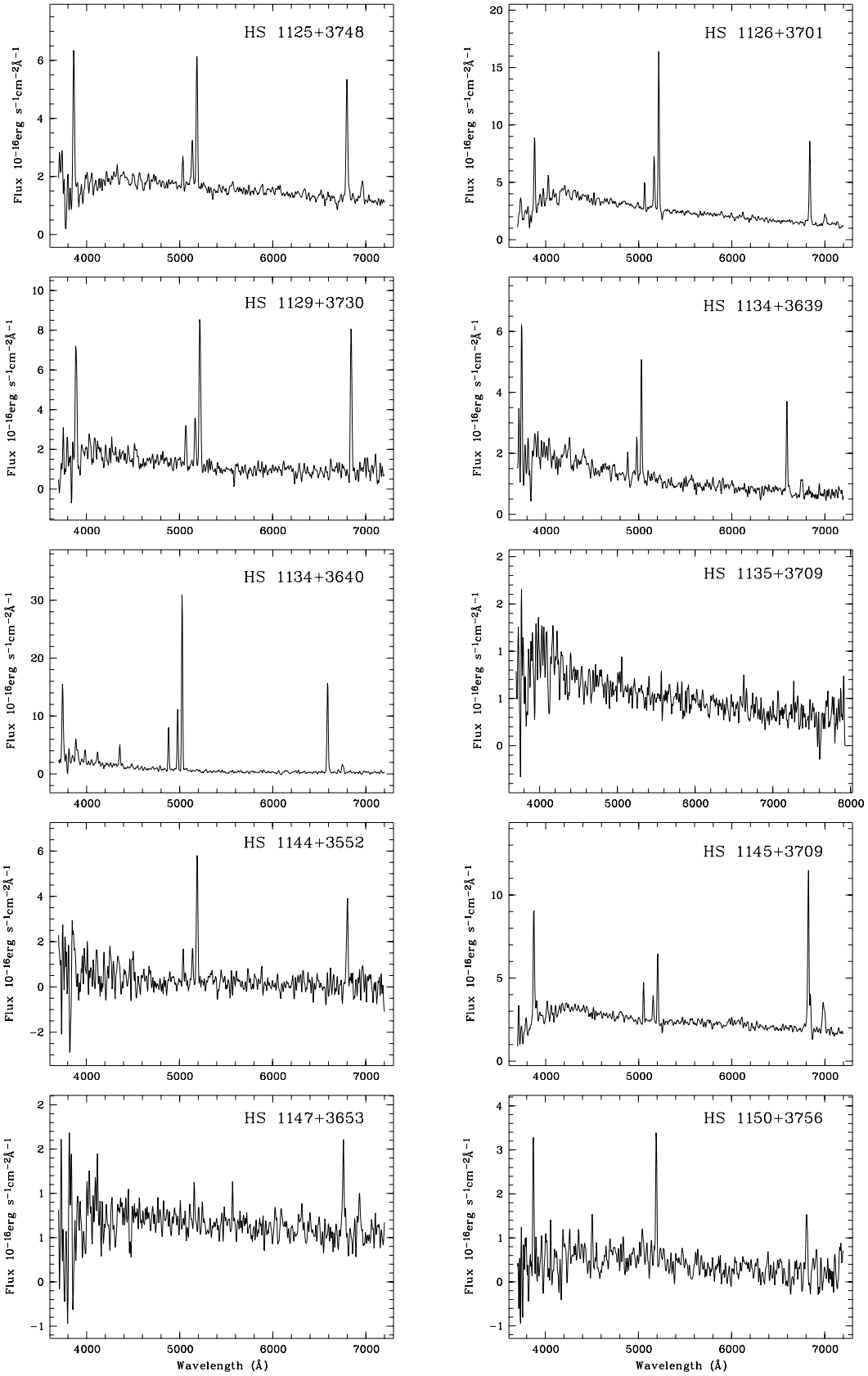
HS 1125+3748
HS 1126+3701
HS 1129+3730
HS 1134+3639
HS 1134+3640
HS 1135+3709
HS 1144+3552
HS 1145+3709
HS 1147+3653
HS 1150+3756
Flux 10⁻¹⁶erg s⁻¹cm⁻²Å⁻¹
Wavelength (Å)

Fig. A7.

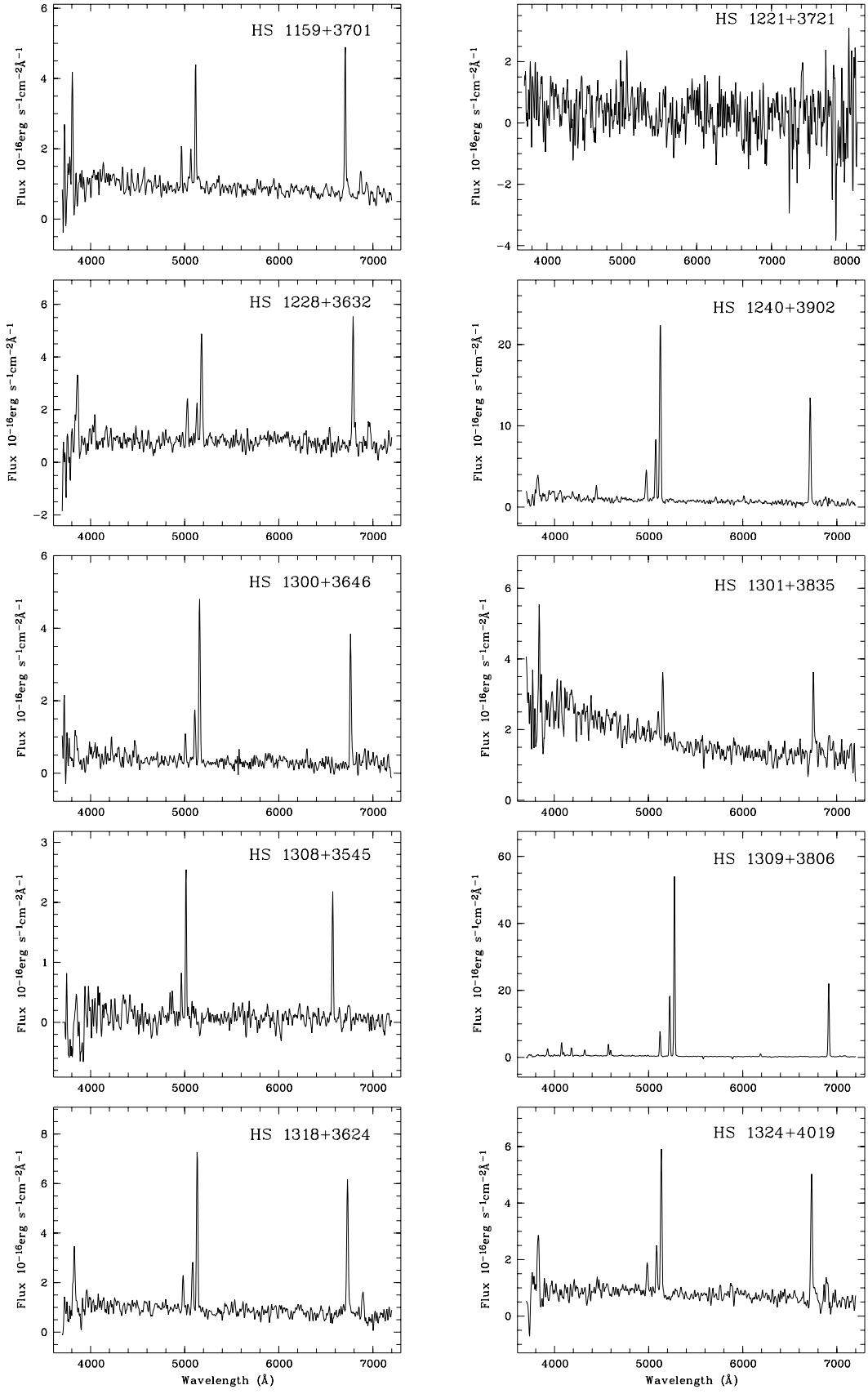
HS 1159+3701
HS 1221+3721
HS 1228+3632
HS 1240+3902
HS 1300+3646
HS 1301+3835
HS 1308+3545
HS 1309+3806
HS 1318+3624
HS 1324+4019
Flux 10⁻¹⁶erg s⁻¹cm⁻²Å⁻¹
Wavelength (Å)

Fig. A8.

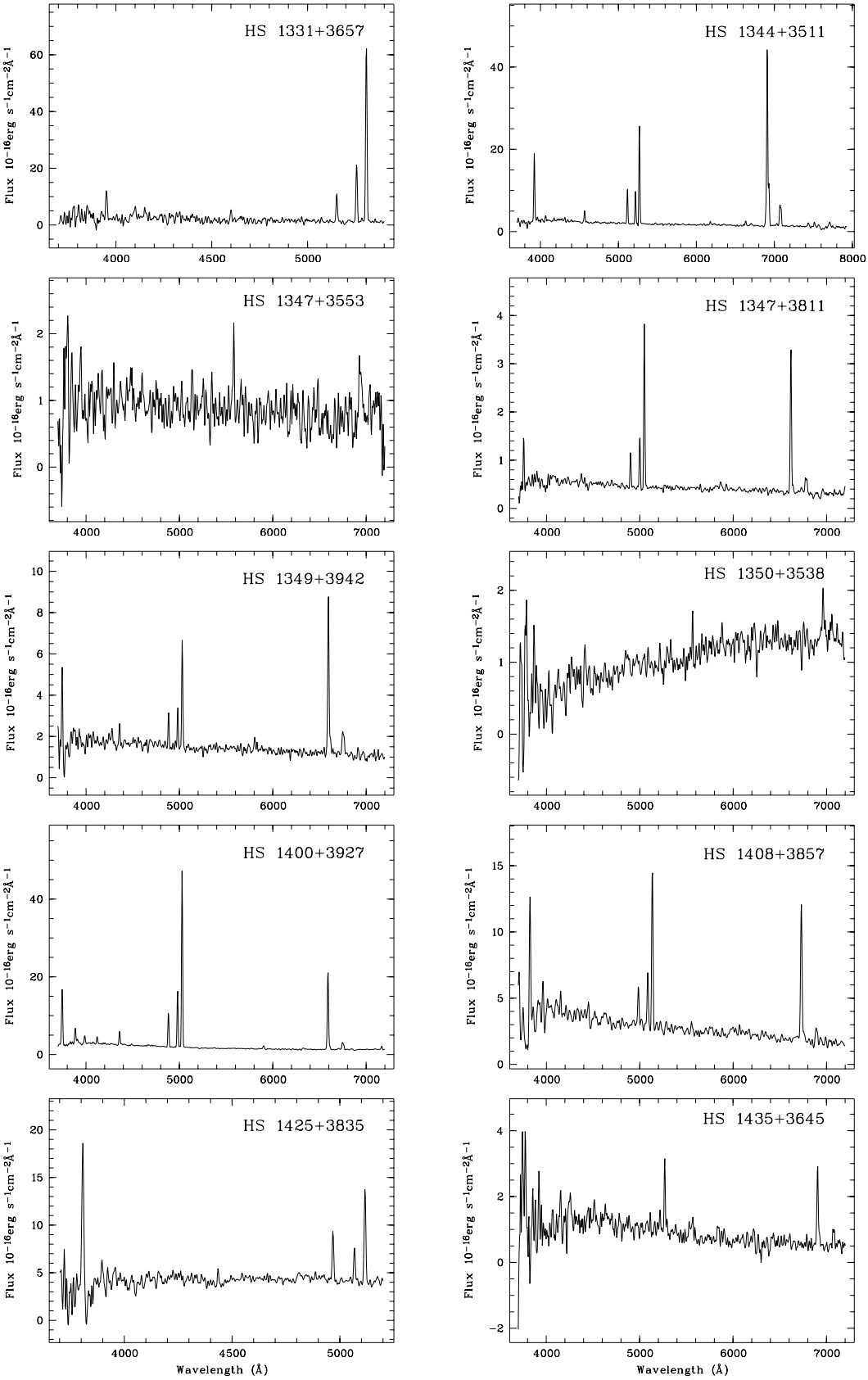
HS 1331+3657
HS 1344+3511
HS 1347+3553
HS 1347+3811
HS 1349+3942
HS 1350+3538
HS 1400+3927
HS 1408+3857
HS 1425+3835
HS 1435+3645
Flux 10⁻¹⁶erg s⁻¹cm⁻²Å⁻¹
Wavelength (Å)

Fig. A9.

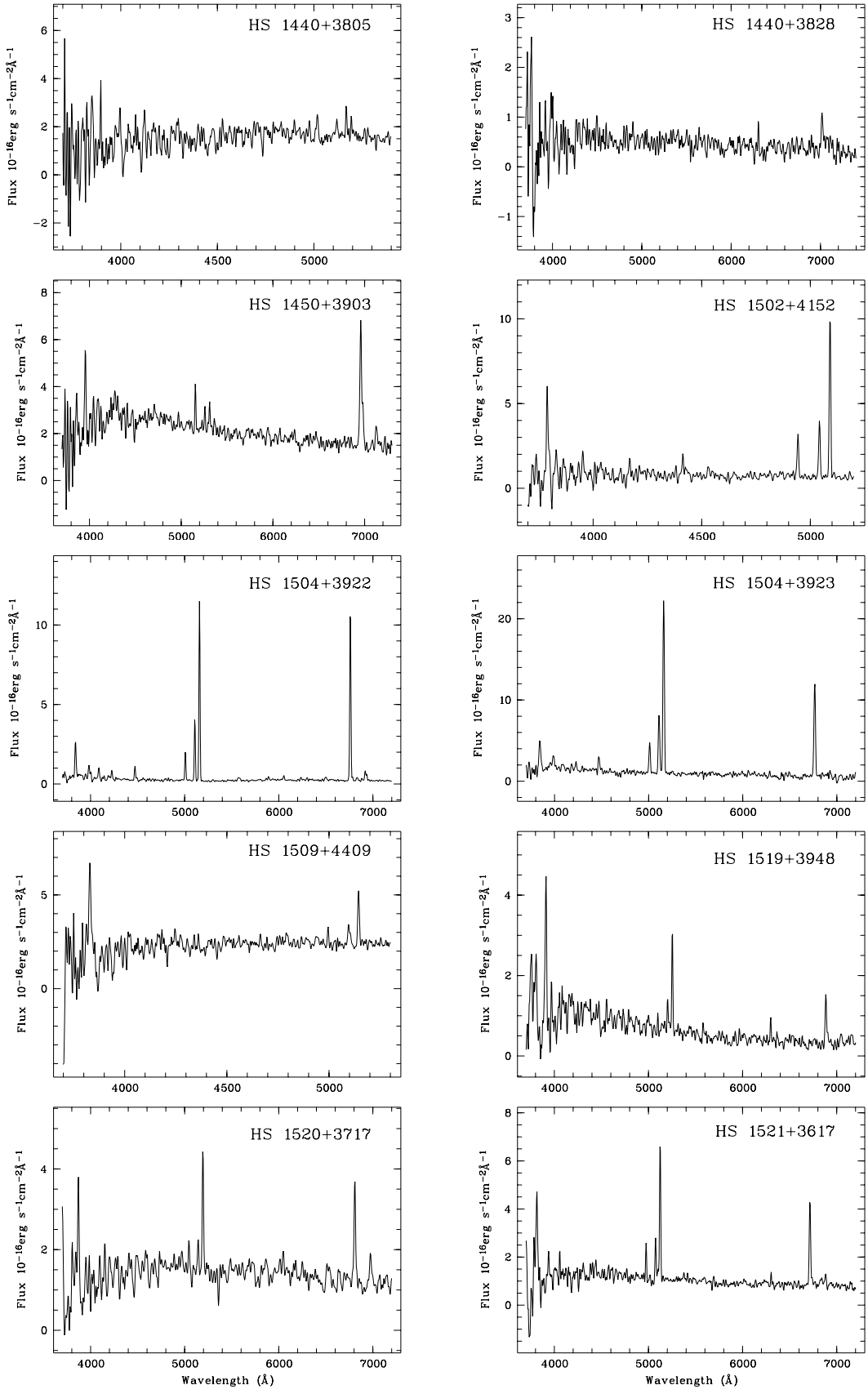
HS 1440+3805
HS 1440+3828
HS 1450+3903
HS 1502+4152
HS 1504+3922
HS 1504+3923
HS 1509+4409
HS 1519+3948
HS 1520+3717
HS 1521+3617
Flux 10⁻¹⁶erg s⁻¹cm⁻²Å⁻¹
Wavelength (Å)

Fig. A10.

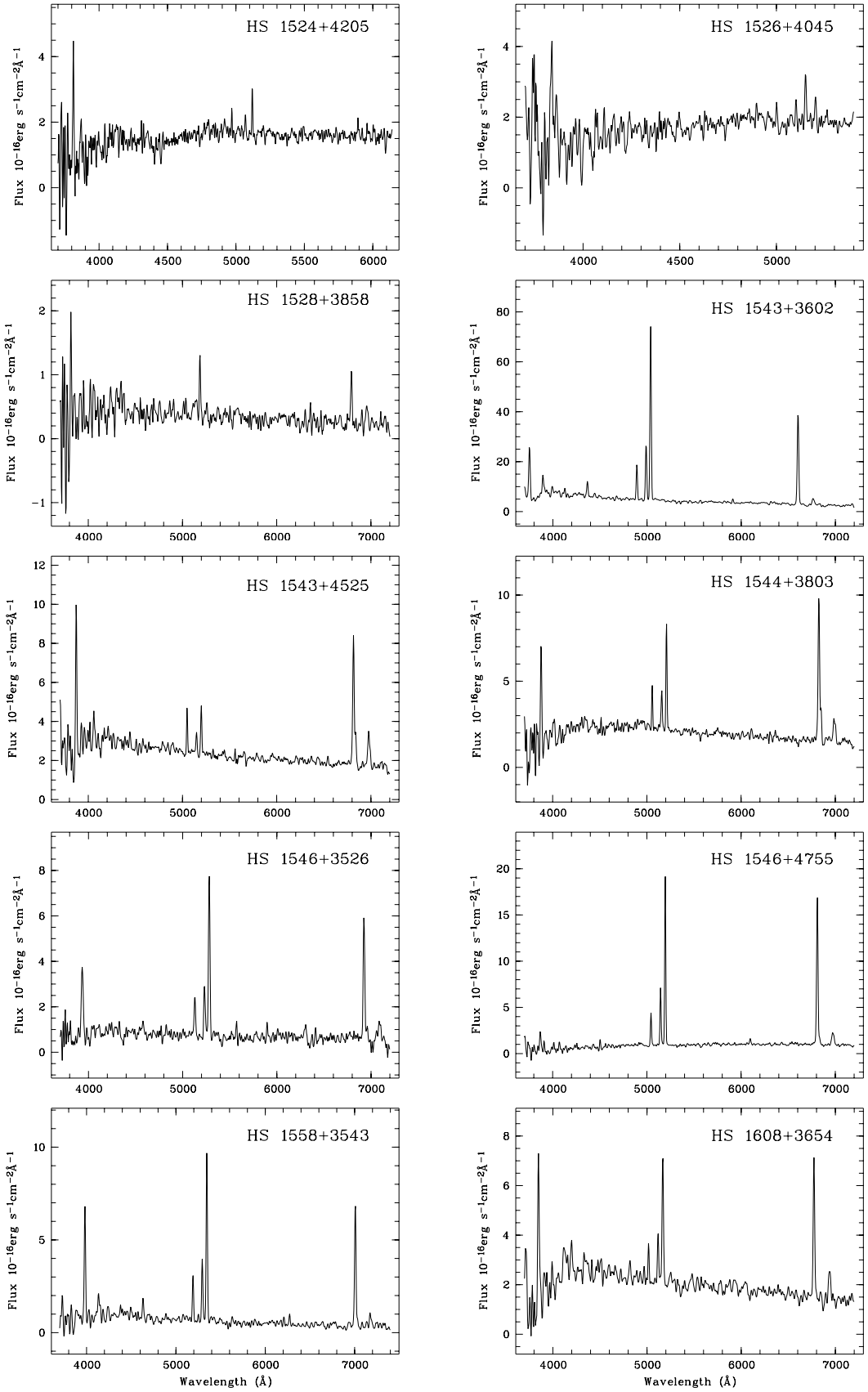
HS 1524+4205
HS 1526+4045
HS 1528+3858
HS 1543+3602
HS 1543+4525
HS 1544+3803
HS 1546+3526
HS 1546+4755
HS 1558+3543
HS 1608+3654
Flux 10⁻¹⁶erg s⁻¹cm⁻²Å⁻¹
Wavelength (Å)

Fig. A11.